

## Chapter 4

### **Fluorescent probes for cytochrome P450 structural characterization and inhibitor screening<sup>†</sup>**

<sup>†</sup>Adapted from: Dunn, A. R.; Hays, A.-M. A.; Goodin, D. B; Stout, C. D.; Chiu, R.; Winkler, J. R.; Gray, H. B. *J. Am. Chem. Soc.*, **2002**, *124*, 10254-10255.

#### *Acknowledgements:*

The synthesis and spectroscopy discussed in this paper were performed in collaboration with Richard Chiu. The crystal structures of P450cam:danysl probe conjugates were determined by Anna-Maria Hays, David Goodin, and C. David Stout.

**ABSTRACT**

We have synthesized two dansyl-based luminescent probes (D-4-Ad and D-8-Ad) that target cytochrome P450cam. D-4-Ad luminescence is quenched by Förster energy transfer upon binding ( $K_d = 0.83 \mu\text{M}$ ), but is restored when the probe is displaced from the active site by camphor. In contrast, D-8-Ad ( $K_d \sim 0.02 \mu\text{M}$ ) is not displaced from the enzyme even in the presence of a large excess of camphor. The 2.2 Å resolution crystal structure of the D-8-Ad:P450cam complex reveals extensive hydrophobic contacts between the probe and the enzyme, which result from the conformational flexibility of the B', F and G helices. Probes with properties similar to those of D-4-Ad potentially could be useful for screening P450 inhibitors.

## INTRODUCTION

Substrate-specific cytochromes P450 play major roles in steroid and eicosanoid biosynthesis, and thus constitute important drug design targets.<sup>1</sup> In contrast, P450 isozymes expressed in the liver take part in the metabolism of nearly all drugs.<sup>2</sup> Adverse drug reactions, for instance to Prozac,<sup>3</sup> result from individual variations in hepatic P450s.<sup>4</sup> It is thus important to predict which P450s interact with a potential drug candidate, and to understand the nature of these interactions.

We have developed fluorescent probe molecules for P450cam that consist of an  $\alpha,\omega$ -diaminoalkane chain connecting a dansyl fluorophore to the P450cam substrate adamantane (Scheme 4.1). The synthesis of the dansyl-substrates was designed to be short, robust, and modular for maximum ease and flexibility. A shift in Soret absorption (Figure 4.1) as well as greatly diminished dansyl luminescence attributable to Förster energy transfer to the heme<sup>5</sup> (Figure 4.2) accompany probe binding. When D-4-Ad is displaced from the active site by camphor, fluorescence is restored (Figure 4.2a).<sup>6</sup> Because a bright signal stands out against a dark background, substrate or inhibitor binding is readily detected. This assay, which is both simple and sensitive, can be employed to screen combinatorial chemical libraries.<sup>7</sup>

**Scheme 4.1.** (A) Dansyl-based fluorescent probe molecules used in this study. (B)

Synthesis of D-4-Ad.

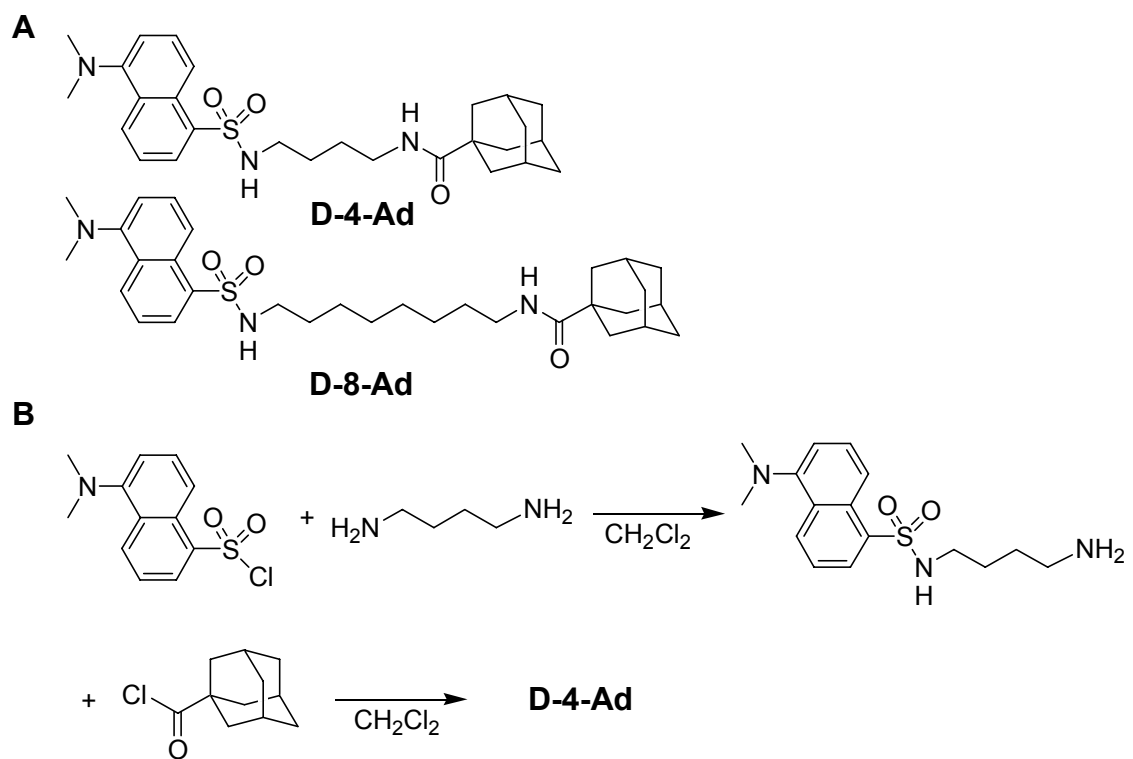


**Figure 4.1.** (A) Absorption spectra showing the binding of camphor to P450cam (4.9  $\mu\text{M}$ ) in the presence of 1 equivalent of D-4-Ad. The initial addition of D-4-Ad to P450cam results in a shift in the Soret from 416 to 414 nm. A fit of the data to a competitive binding model gives a dissociation constant of 0.83  $\mu\text{M}$ . (B) The camphor-induced shift from low- to high-spin P450cam (5.7  $\mu\text{M}$ ) in the presence of 1 equivalent of D-8-Ad. Black, P450cam; purple, P450cam + 1 equivalent dansyl probe; blue to red, 0.5, 1, 2, 4, 8, 16, 32, and 64 equivalents camphor.

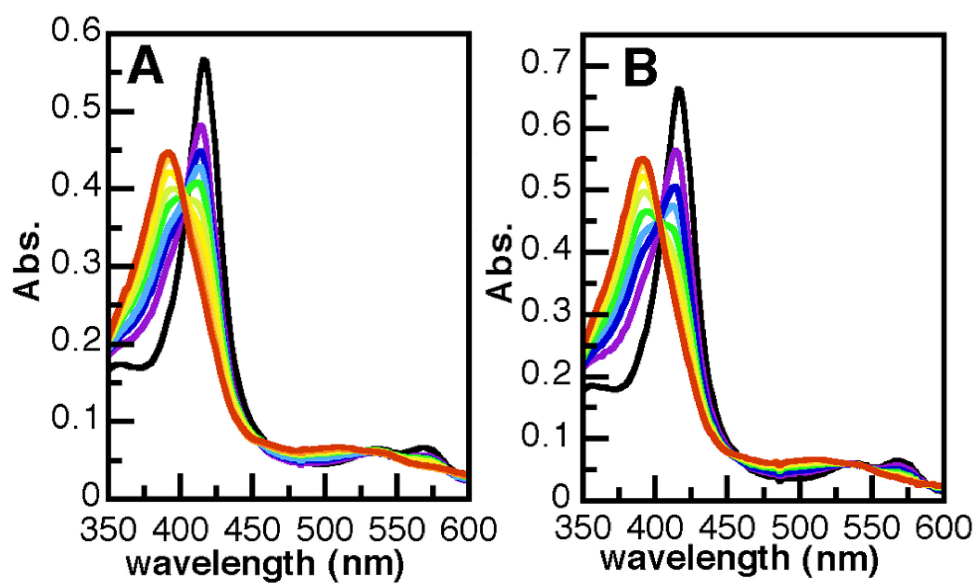
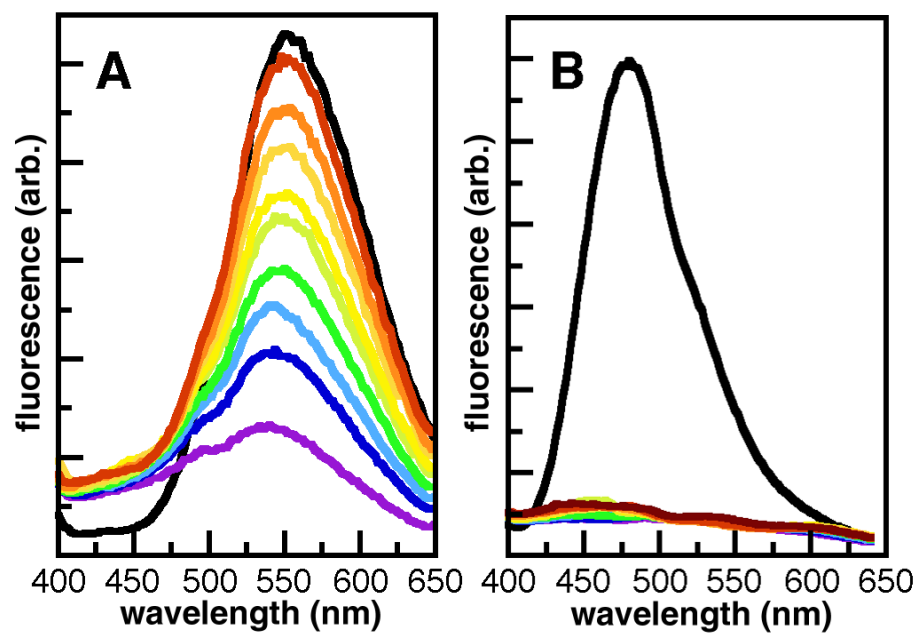


**Figure 4.2.** Fluorescence spectra of D-4-Ad (A) and D-8-Ad (B). Black, 2  $\mu\text{M}$  D-8-Ad or D-4-Ad; purple, 2  $\mu\text{M}$  dansyl probe + 1 equivalent P450cam; blue to red: 2  $\mu\text{M}$  P450cam and dansyl probe + 0.5, 1, 2, 4, 8, 16, 32, and 64 equivalents of camphor ( $K_d=1.6 \mu\text{M}$ ).<sup>8</sup>





## MATERIALS AND METHODS

P450cam was expressed and purified as previously described.<sup>9</sup> Steady-state UV-visible absorption spectra were measured on a Hewlett Packard 8452A diode array spectrophotometer. Steady-state fluorescence spectra were measured using an ISS K2 fluorometer ( $\lambda_{\text{ex}} = 340 \text{ nm}$ ). Absorption and emission spectra were collected in quartz cuvettes using 50 mM potassium phosphate buffer (pH 7.4) containing 100 mM KCl. NMR spectra were collected on an Oxford Instruments 300 MHz NMR and analyzed with Varian VNMR 6.1B software. Electrospray mass spectra were collected on a Finnigan LCQ ion trap mass spectrometer. Buried solvent accessible surface area was calculated using the solvation module of InsightII (1.4 Å radius probe). All reagents were purchased from the Aldrich chemical company and used as received. DMF and N,N-diisopropylethylamine were anhydrous, and used as received.

## RESULTS AND DISCUSSION

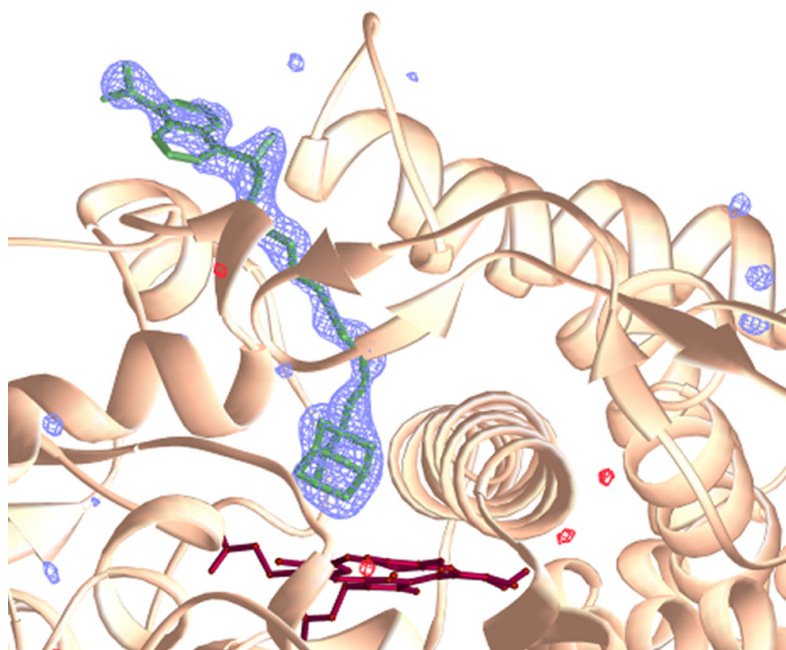
Both fluorescence and absorption spectra show that D-4-Ad binding to P450cam is competitive with camphor. The Soret shift (416 to 414 nm) induced by D-4-Ad indicates that it binds in the active site. With a  $K_d$  of 0.83  $\mu\text{M}$ , D-4-Ad binds twice as strongly as the natural substrate. D-8-Ad also induces a shift in the Soret maximum from 416 to 414 nm: from the integrated D-8-Ad fluorescence in the presence and absence of P450cam, we estimate an upper limit  $K_d \sim 0.02 \mu\text{M}$  for this probe.

Interestingly, the titration of a 1:1 mixture of D-8-Ad and P450cam with camphor also shows a shift in the Soret to 392 nm, and an *apparent* camphor  $K_d$  of  $\sim 1 \mu\text{M}$  (Figure 4.1B). However, the steady-state luminescence titrations indicate that D-8-Ad remains bound to P450cam even when the absorption spectrum indicates that the heme has converted fully to its high spin, and presumably camphor-bound, form. The luminescence and absorption data are best reconciled by a model that includes simultaneous camphor and D-8-Ad binding. Given the low  $K_d$  of D-8-Ad, it is perhaps not surprising that camphor binding fails to expel the probe into solution.

The crystal structure of the P450cam:D-8-Ad complex shows that the probe binds in the same channel as  $\text{Ru}^{\text{II}}(\text{bpy})_3$ -linker-Ad (bpy = 2,2'-bipyridine) analogs (Figure 4.3).<sup>9,10</sup> The eight-carbon chain is nearly fully extended, allowing the dansyl moiety to bind at the surface of the protein. The good fit is attributable to conformational flexibility, that is, the F and G helices open just enough to allow the probe to enter and bind. The observed conformation is midway between the “closed” (camphor)<sup>11</sup> and “open” (Ru-linker-Ad)<sup>10c</sup> structures.

The structure reveals a hydrogen bond between the amide carbonyl of the probe and Tyr96 in P450cam:D-8-Ad, mimicking the hydrogen bond between camphor and Tyr96 in the P450cam:substrate complex.<sup>11</sup> In addition, there are a great many hydrophobic interactions between the probe molecule and the enzyme; analysis of these

**Figure 4.3.** The 2.2 Å resolution structure of the D-8-Ad:P450cam cocrystal, with the omit electron density ( $|F_{\text{obs}}| - |F_{\text{calc}}|$ ) contoured at 4.0  $\sigma$  (blue positive, red negative).

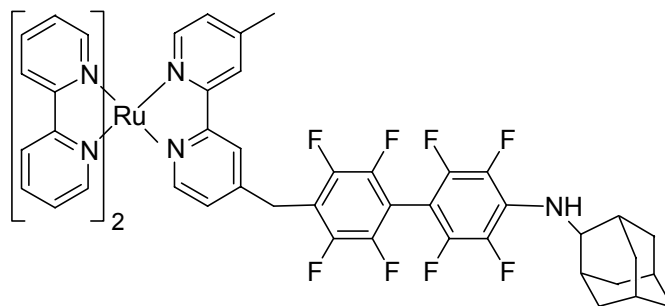
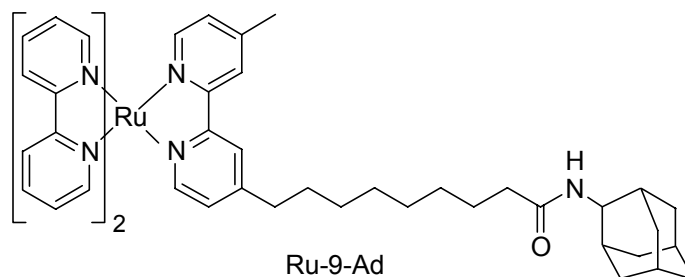


contacts shows that much of the solvent accessible surface area is buried. The estimated  $K_d$  of 0.02  $\mu\text{M}$  corresponds to a binding energy of  $\sim 11$  kcal/mol, or  $\sim 11$  cal/mol  $\text{\AA}^2$  (Figure 4.4). The  $\text{Ru}(\text{bpy})_3^{2+}$  analogs (Ru-9-Ad and Ru-F<sub>8</sub>bp-Ad) do not bind as tightly to P450cam, but the free energy changes per buried surface area are comparable.

The structure of the D-4-Ad:P450cam complex shows the enzyme in a conformation similar to that observed in the P450cam:Ru-wire conjugates (Figure 4.5). The shorter D-4-Ad hydrocarbon tether results in dansyl moiety occupying the relatively narrow “neck” of the substrate access channel, thus capturing the enzyme in a relatively more open conformation. This inferior steric fit as compared to the D-8-Ad:P450cam structure likely is responsible for the differences in binding constants observed for D-4-Ad and D-8-Ad.

In addition, a preliminary structure of the ternary P450cam:D-8-Ad:camphor complex has recently been determined. Initial analysis based on partial refinement of this data indicates that D-8-Ad remains bound in the active site and substrate access channel.<sup>12</sup> Importantly, the F and G helices adopt a opened conformation akin to the Ru-wire bound structures, and markedly different than that observed in the D-8-Ad:P450cam conjugate structure. In addition, the B' helix and loop form a greatly altered conformation somewhat analogous to that seen in the Ru-F<sub>8</sub>bp-Ad:P450cam structure.

**Figure 4.4.** (top) Ruthenium *tris*-bipyridyl photosensitizers known to bind P450cam. The crystal structures of both compounds bound to P450cam have been determined to high resolution (Ru-9-Ad 1.55 Å, Ru-F<sub>8</sub>bp-Ad 1.65 Å).<sup>10c</sup> (bottom) Dissociation constants, binding energies, buried solvent accessible surface areas (SASA) and the binding energy per square angstrom of buried surface area for the P450cam:probe complexes. The Ru-9-Ad:P450cam crystal contains both  $\Delta$  and  $\Lambda$  stereoisomers.

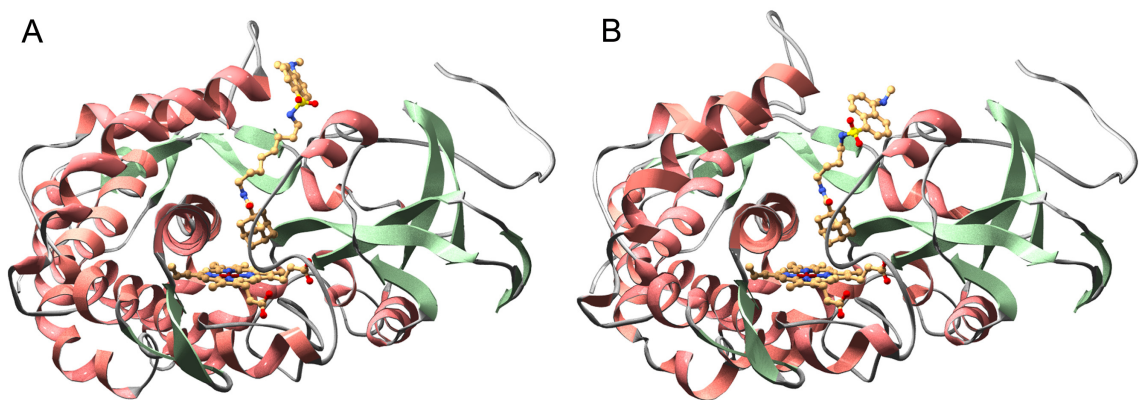
Ru-F<sub>8</sub>bp-Ad

Ru-9-Ad

Compound	K <sub>d</sub> (nM)	kcal mol <sup>-1</sup>	Buried SASA (Å <sup>2</sup> )	cal mol <sup>-1</sup> Å <sup>-2</sup>
<b>D-8-Ad</b>	~20	~11	988	~11
<b>Ru-9-Ad (Δ)</b>	190	9.23	1097	8.4
<b>Ru-9-Ad (Λ)</b>	90	9.69	1042	9.3
<b>Ru-F<sub>8</sub>bp-Ad</b>	74	9.80	1191	8.2



**Figure 4.5.** (A) Ribbon diagram of the D-8-Ad:P450cam crystal structure. (B) Ribbon diagram of the D-4-Ad:P450cam crystal structure; note the wider substrate access channel, and the deeper position of the dansyl moiety within the channel.



These provisional data demonstrate unambiguously that P450cam binds camphor and D-8-Ad simultaneously.

### **CONCLUDING REMARKS**

Even though P450cam has evolved for a single, relatively small substrate, it has the ability to bind much larger molecules more tightly. The key to this ability is the mobility of the B', F, and G helices (Chapter 3).<sup>10c</sup> Both solution<sup>13</sup> and crystallographic<sup>14</sup> studies of other P450s suggest that this feature is common to the P450 superfamily. The two probes described herein illustrate the usefulness of our methodology. D-4-Ad can be employed to screen potential P450 inhibitors, as it is easily displaced by other molecules with comparable or lower dissociation constants. In contrast, D-8-Ad binds extremely tightly: the conformational flexibility of the P450 fold allows the enzyme to close around the probe, thereby making a great many productive hydrophobic contacts. The insight gained from the D-8-Ad:P450cam structure could potentially lead to a more rational design strategy for P450 inhibitors.

### **ACKNOWLEDGEMENT**

This work was supported by the Fannie and John Hertz Foundation (ARD), the National Science Foundation, and the National Institutes of Health (Metalloprotein Program Project Grant P01 GM48495; NRSA fellowship GM20703 to A-MAH).

## REFERENCES AND NOTES

1. (a) Kagawa, N.; Waterman, M. R. In *Cytochrome P450: Structure, Mechanism and Biochemistry*; Ortiz de Montellano, P. R., Ed.; Plenum Press: New York, 1995, pp 419-442. (b) Capdevila, J. H.; Zeldin, D.; Makita, K.; Karara, A.; Falck, J. R. In *Cytochrome P450: Structure, Mechanism and Biochemistry*; Ortiz de Montellano, P. R., Ed.; Plenum Press: New York, 1995, pp 443-472. (c) Goss, P. E.; Strasser, K. *J. Clin. Oncol.* **2001**, *19*, 881-94. (d) Frye, L. L.; Leonard, D. A. *Crit. Rev. Biochem. Mol. Biol.* **1999**, *34*, 123-140. (e) Sheehan, D. J.; Hitchcock, C. A.; Sibley, C. M. *Clin. Microbiol. Rev.* **1999**, *12*, 40-79.
2. (a) Rendic, S.; DiCarlo, F. J. *Drug Metab. Rev.* **1997**, *29*, 413-580. (b) Guengerich, F. P. In *Cytochrome P450: Structure, Mechanism and Biochemistry*; Ortiz de Montellano, P. R., Ed.; Plenum Press: New York, NY, 1995, pp 473-536.
3. Otton, S. V.; Wu, D. F.; Joffe, R. T.; Cheung, S. W.; Sellers, E. M. *Clin. Pharm. Ther.* **1993**, *53*, 401-409.
4. Li, A. P. *Drug-drug interactions: scientific and regulatory perspectives*; Academic Press: New York, 1997; Vol. 21, pp 304
5. (a) Wu, P.; Brand, L. *Anal. Biochem.* **1994**, *218*, 1-13. (b) Selvin, P. R. *Nature Struct. Biol.* **2000**, *7*, 730-734.

6. The fluorescence of D-8-Ad ( $\lambda_{\max}$  480 nm) is blue shifted from that of D-4-Ad (550 nm), indicating that the D-8-Ad environment is less polar [Li, Y.-H.; Chan, L.-M.; Tyer, L.; Moody, R. T.; Himel, C. M.; Hercules, D. M. *J. Am. Chem. Soc.* **1975**, *97*, 3118-3126]. One possible explanation is that the hydrophobic tail of D-8-Ad folds back in solution to partially cover the dansyl fluorophore, effectively lowering the local dielectric. Although the fluorescence maximum is not concentration dependent (data not shown), D-8-Ad aggregation cannot be ruled out.
7. Schobel, U.; Coille, I.; Brecht, A.; Steinwand, M.; Gauglitz, G. *Anal. Chem.* **2001**, *73*, 5172-5179.
8. Atkins, W. M.; Sligar, S. G. *J. Biol. Chem.* **1988**, *263*, 18842-18849.
9. Dmochowski, I. J.; Crane, B. R.; Wilker, J. J.; Winkler, J. R.; Gray, H. B. *Proc. Natl. Acad. Sci. USA* **1999**, *23*, 12987-12990.
10. (a) Wilker, J. J.; Dmochowski, I. J.; Dawson, J. H.; Winkler, J. R.; Gray, H. B. *Angew. Chem., Int. Ed. Engl.* **1999**, *38*, 90-92. (b) Dmochowski, I. J.; Crane, B. R.; Wilker, J. J.; Winkler, J. R.; Gray, H. B. *Proc. Natl. Acad. Sci. USA* **1999**, *23*, 12987-12990. (c) Dunn, A. R.; Dmochowski, I. J.; Bilwes, A. M.; Gray, H. B.; Crane, B. R. *Proc. Natl. Acad. Sci. USA* **2001**, *98*, 12420-12425.

11. Poulos, T. L.; Finzel, B. C.; Howard, A. J. *J. Mol. Biol.* **1987**, *195*, 867-700.
12. Anna-Maria A. Hays, personal communication.
13. (a) DiPrimo, C.; Hoa, G. H. B.; Deprez, E.; Douzou, P.; Sligar, S. G. *Biochemistry* **1993**, *32*, 3671-3676. (b) Prasad, S.; Mazumdar, S.; Mitra, S. *FEBS Lett.* **2000**, *477*, 157-160. (c) Lepesheva, G. I.; Strushkevich, N. V.; Usanov, S. A. *Biochem. Biophys. Acta* **1999**, *1434*, 31-43.
14. (a) Li, H.; Poulos, T. L. *Biochim. Biophys. Acta* **1999**, *1441*, 141-149. (b) Ravichandran, K. G.; Boddupalli, S. S.; Hasemann, C. A.; Peterson, J. A.; Deisenhofer, J. *Science* **1993**, *261*, 731-736. (c) Hasemann, C. A.; Ravichandran, K. G.; Peterson, J. A.; Deisenhofer, J. *J. Mol. Biol.* **1994**, *236*, 1169-1185. (d) Williams, P. A.; Cosme, J.; Sridhar, V.; Johnson, E. F.; McRee, D. E. *Mol. Cell* **2000**, *5*, 121-131. (e) Yano, J. K.; Koo, L. S.; Schuller, D. J.; Li, H.; Ortiz de Montellano, P. R.; Poulos, T. L. *J. Biol. Chem.* **2000**, *275*, 31086-31092.